INTRODUCTION TO FINITE ELEMENT METHODS

LONG CHEN

Finite element methods are grounded in the variational formulation of partial differential equations. These methods enable the construction of finite element spaces on general triangulations, effectively managing complex geometries and boundaries. Boundary conditions are naturally incorporated into the weak formulation or function space. The variational foundation of these methods facilitates systematic error analysis, making them the preferred choice for elliptic equations in complex domains.

1. Galerkin Methods

The finite element methods have been introduced as methods for approximate solution of variational problems. Let us consider the model problem: Poisson equation with homogenous Dirichlet boundary conditions

$$-\Delta u = f \ \text{ in } \Omega, \qquad u = 0 \ \text{ on } \partial\Omega. \tag{1}$$

Multiply a test function v, integrate over Ω, and use integration by parts to obtain the corresponding variational formulation: Find $u \in V = H_0^1(\Omega) := \{v \in L^2(\Omega) | \nabla v \in L^2(\Omega), v|_\Gamma = 0\}$, such that

$$a(u, v) = (f, v), \quad \text{for all } \ v \in V. \tag{2}$$

where

$$a(u, v) = \int_\Omega \nabla u \cdot \nabla v \,\mathrm{d}x, \quad (f, v) = \int_\Omega f v \,\mathrm{d}x, \quad \text{for } f \in L_2(\Omega)$$

Clearly, in such case $a(\cdot, \cdot)$ is bilinear and symmetric, and $a(u, u) = |u|_{1,\Omega}^2 := \|\nabla u\|^2$. Furthermore $a(u, u) = 0$ implies $\nabla u = 0$ and consequently u is constant. As $u|_\Gamma = 0$, this constant should be zero. Therefore $a(\cdot, \cdot)$ defines an inner product on V, and thus the problem (2) has a unique solution by the Riesz representation theorem.

We now consider a class of methods, known as *Galerkin methods* which are used to approximate the solution to (2). Consider a finite dimensional subspace $V_h \subset V$. Restrict the variational form in the subspace V_h, i.e., find $u_h \in V_h$ s.t.

$$a(u_h, v_h) = (f, v_h) \quad \text{for all } v_h \in V_h. \tag{3}$$

Let $V_h = \operatorname{span}\{\phi_1, \ldots, \phi_N\}$. For any function $v \in V_h$, there is a unique representation: $v = \sum_{i=1}^N v_i \phi_i$. We thus can define an isomorphism $V_h \cong \mathbb{R}^N$ by

$$v = \sum_{i=1}^N v_i \phi_i \longleftrightarrow \boldsymbol{v} = (v_1, \cdots, v_N)^\intercal,$$

and call $\boldsymbol{v}$ the coordinate vector of v relative to the basis $\{\phi_i\}_{i=1}^N$. Following the terminology in elasticity, we introduce the *stiffness matrix*

$$\boldsymbol{A} = (a_{ij})_{N\times N}, \ \text{ with } \quad a_{ij} = a(\phi_j, \phi_i),$$

Date: Created on Oct 2007. Latest update January 17, 2024.

and the *load vector* $\boldsymbol{f} = \{\langle f, \phi_k\rangle\}_{k=1}^N \in \mathbb{R}^N$. Then the variational problem (20) on V_h can be formulated as the following linear algebraic system

$$\boldsymbol{A}\boldsymbol{u} = \boldsymbol{f}.$$

By definition, for two functions $u, v \in V_h$, their $a(\cdot,\cdot)$-inner product is realized by the matrix product

$$a(u_h, v_h) = a\left(\sum_i u_i\phi_i, \sum v_j\phi_j\right) = \sum_{i,j} a(\phi_i,\phi_j) u_i\, v_j = \boldsymbol{v}^{\intercal}\boldsymbol{A}\boldsymbol{u}. \tag{4}$$

Therefore for any vector $\boldsymbol{u} \in \mathbb{R}^N, \boldsymbol{u}^{\intercal}\boldsymbol{A}\boldsymbol{u} = a(u,u) \geq 0$ and equals 0 if and only if $\boldsymbol{u}$ is zero. Namely $\boldsymbol{A}$ is an SPD matrix and thus the solution $\boldsymbol{u} = \boldsymbol{A}^{-1}\boldsymbol{f}$ exists and unique. After we get the coefficient vector $\boldsymbol{u}$, u_h can be obtained by linear combination of basis functions.

The finite element method, a prominent and widely-used example of Galerkin methods, constructs a finite-dimensional subspace V_h based on triangulations $\mathcal{T}_h$ of the domain. The name comes from the fact that the domain is decomposed into finite number of elements. Usually piecewise polynomials are used to define a finite dimensional space.

2. Triangulations and Barycentric Coordinates

In this section, we discuss triangulations used in finite element methods. We would like to distinguish two structures related to a triangulation: one is the topology of a mesh determined by the combinatorial connectivity of vertices; another is the geometric shape which depends on both the connectivity and the location of vertices.

2.1. **Geometric simplex and triangulation.** Let $\boldsymbol{x}_i = (x_{1,i}, \cdots, x_{n,i})^{\intercal}, i = 1, \cdots, n+1$ be $n+1$ points in $\mathbb{R}^n$. We say $\boldsymbol{x}_1, \cdots, \boldsymbol{x}_{n+1}$ do not all lie in one hyper-plane if the n-vectors $\boldsymbol{x}_1\boldsymbol{x}_2, \cdots, \boldsymbol{x}_1\boldsymbol{x}_{n+1}$ are independent. This is equivalent to the matrix:

$$A = \begin{pmatrix} x_{1,1} & x_{1,2} & \dots & x_{1,n+1} \\ x_{2,1} & x_{2,2} & \dots & x_{2,n+1} \\ \vdots & \vdots & & \vdots \\ x_{n,1} & x_{n,2} & \dots & x_{n,n+1} \\ 1 & 1 & \dots & 1 \end{pmatrix}$$

is non-singular. Given any point $\boldsymbol{x} = (x_1, \cdots, x_n) \in \mathbb{R}^n$, by solving the following linear system

$$A\begin{pmatrix} \lambda_1 \\ \vdots \\ \lambda_n \\ \lambda_{n+1} \end{pmatrix} = \begin{pmatrix} x_1 \\ \vdots \\ x_n \\ 1 \end{pmatrix}, \tag{5}$$

we obtain unique $n+1$ real numbers $\lambda_i(\boldsymbol{x}), 1 \leq i \leq n+1$, such that for any $\boldsymbol{x} \in \mathbb{R}^n$

$$\boldsymbol{x} = \sum_{i=1}^{n+1} \lambda_i(\boldsymbol{x})\boldsymbol{x}_i, \quad \text{with} \quad \sum_{i=1}^{n+1}\lambda_i(\boldsymbol{x}) = 1. \tag{6}$$

The *convex hull* of the $d+1$ points $\boldsymbol{x}_1, \cdots, \boldsymbol{x}_{d+1}$ in $\mathbb{R}^n$

$$\tau := \{\boldsymbol{x} = \sum_{i=1}^{d+1} \lambda_i\boldsymbol{x}_i \,|\, 0 \leq \lambda_i \leq 1, i = 1 : d+1, \sum_{i=1}^{d+1}\lambda_i = 1\} \tag{7}$$

is defined as a *geometric d-simplex* generated (or spanned) by the vertices $\boldsymbol{x}_1, \cdots, \boldsymbol{x}_{d+1}$. For example, a triangle is a 2-simplex and a tetrahedron is a 3-simplex. For an integer $0 \leq m \leq d-1$, an m-dimensional face of τ is any m-simplex generated by $m+1$ vertices of τ. Zero dimensional faces are vertices and one-dimensional faces are called edges of τ. The $(d-1)$-face opposite to the vertex $\boldsymbol{x}_i$ will be denoted by F_i.

The numbers $\lambda_1(\boldsymbol{x}), \cdots, \lambda_{d+1}(\boldsymbol{x})$ are called *barycentric coordinates* of $\boldsymbol{x}$ with respect to the $d+1$ points $\boldsymbol{x}_1, \cdots, \boldsymbol{x}_{d+1}$. There is a simple geometric meaning of the barycentric coordinates. Given a $\boldsymbol{x} \in \tau$, let $\tau_i(\boldsymbol{x})$ be the simplex with vertices $\boldsymbol{x}_i$ replaced by $\boldsymbol{x}$. Then, by the Cramer's rule for solving (5),

$$\lambda_i(\boldsymbol{x}) = \frac{|\tau_i(\boldsymbol{x})|}{|\tau|}, \tag{8}$$

where $|\cdot|$ is the Lebesgue measure in $\mathbb{R}^d$, namely area in two dimensions and volume in three dimensions. Note that $\lambda_i(\boldsymbol{x})$ is an affine function of $\boldsymbol{x}$ and vanished on the face F_i.

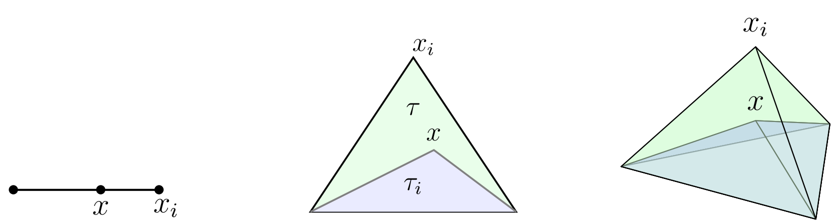

(a) 1d simplex (b) 2d simplex (c) 3d simplex

FIGURE 1. Geometric explanation of barycentric coordinates.

It is convenient to have a standard simplex $s^n \subset \mathbb{R}^n$ spanned by the vertices $\boldsymbol{0}, \boldsymbol{e}_1, \cdots, \boldsymbol{e}_n$ where $\boldsymbol{e}_i = (0, \cdots, 1, \cdots, 0)$. Then any n-simplex $\tau \subset \mathbb{R}^n$ can be thought as an image of s^n through an affine map $B : s^n \to \tau$ with $B(\boldsymbol{e}_i) = \boldsymbol{x}_i$. See Figure 2. The simplex s^n is also often called the *reference simplex*.

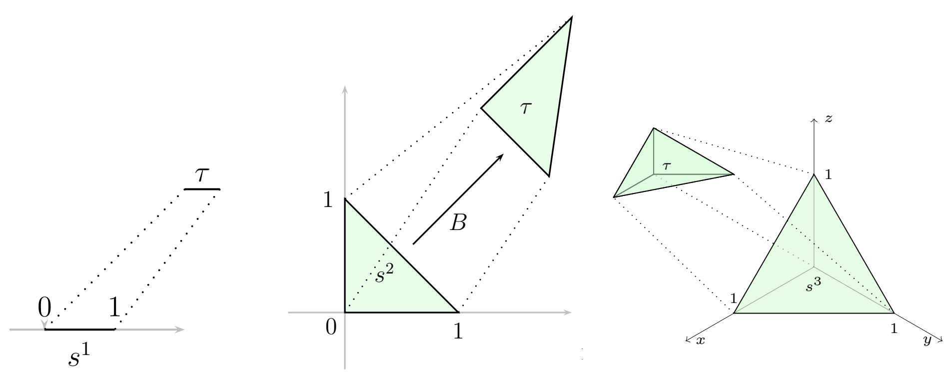

(a) A standard simplex in $\mathbb{R}^1$ (b) A standard simplex in $\mathbb{R}^2$ (c) A standard simplex in $\mathbb{R}^3$

FIGURE 2. Reference simplexes in $\mathbb{R}^1, \mathbb{R}^2$ and $\mathbb{R}^3$.

Let Ω be a polyhedral domain in $\mathbb{R}^d, d \geq 1$. A geometric triangulation (also called mesh or grid) $\mathcal{T}$ of Ω is a set of d-simplices such that

$$\cup_{\tau \in \mathcal{T}} \tau = \overline{\Omega}, \quad \text{and} \quad \overset{\circ}{\tau}_i \cap \overset{\circ}{\tau}_j = \varnothing, i \neq j.$$

Remark 2.1. In this course, we restrict ourself to simplicial triangulations. There are other type of meshes by partition the domain into quadrilateral (in 2-D), cubes, prisms (in 3-D), or polytopes in general.

There are two conditions that we shall impose on triangulations that are important in the finite element computation. The first requirement is a topological property. A triangulation $\mathcal{T}$ is called *conforming* or *compatible* if the intersection of any two simplexes τ and τ' in $\mathcal{T}$ is either empty or a common lower dimensional simplex.

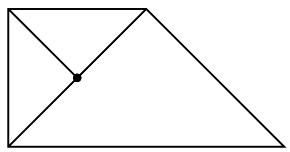

(a) A triangulation with a hanging node

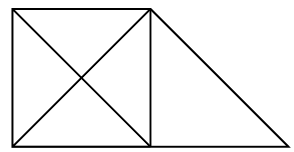

(b) A conforming triangulation

FIGURE 3. Two triangulations. The left is non-conforming and the right is conforming.

The second important condition is on the geometric structure. A set of triangulations $\mathscr{T}$ is called *shape regular* if there exists a constant c_0 such that

$$\max_{\tau \in \mathcal{T}} \frac{\operatorname{diam}(\tau)^d}{|\tau|} \leq c_0, \quad \text{for all } \ \mathcal{T} \in \mathscr{T}, \tag{9}$$

where $\operatorname{diam}(\tau)$ is the diameter of τ and $|\tau|$ is the measure of τ in $\mathbb{R}^d$. In two dimensions, it is equivalent to the minimal angle of each triangulation is bounded below uniformly in the shape regular class. We shall define $h_\tau = |\tau|^{1/n}$ for any $\tau \in \mathcal{T} \in \mathscr{T}$. By (9), $h_\tau \eqsim \operatorname{diam}(\tau)$ represents the size of an element $\tau \in \mathcal{T}$ for a shape regular triangulation $\mathcal{T} \in \mathscr{T}$.

In addition to (9), if

$$\frac{\max_{\tau \in \mathcal{T}} |\tau|}{\min_{\tau \in \mathcal{T}} |\tau|} \leq \rho, \quad \text{for all } \ \mathcal{T} \in \mathscr{T}, \tag{10}$$

$\mathscr{T}$ is called *quasi-uniform*. For quasi-uniform grids, define the mesh size of $\mathcal{T}$ as $h_{\mathcal{T}} := \max_{\tau \in \mathcal{T}} h_\tau$. It is used to measure the approximation rate. In FEM literature, we often write a triangulation as $\mathcal{T}_h$.

2.2. **Abstract simplex and simplicial complex.** To distinguish the topological structure with the geometric one, we now understand the points as abstract entities and introduce *abstract simplex* or *combinatorial simplex*. The set $\tau = \{v_1, \cdots, v_{d+1}\}$ of $d+1$ abstract points is called an abstract d-simplex. A face σ of a simplex τ is a simplex determined by a non-empty subset of τ. A k-face has $k+1$ points. A proper face is any face different from τ.

Let $\mathcal{N} = \{v_1, v_2, \cdots, v_N\}$ be a set of N abstract points. An *abstract simplicial complex* $\mathcal{T}$ is a set of simplices formed by finite subsets of $\mathcal{N}$ such that if $\tau \in \mathcal{T}$ is a simplex, then any face of τ is also a simplex in $\mathcal{T}$. By the definition, a two dimensional combinatorial complex $\mathcal{T}$ contains not only triangles but also edges and vertices of these triangles. A geometric triangulation defined before is only a set of d-simplex not its faces. By including all its face, we shall get a simplicial complex.

A subset $\mathcal{M} \subset \mathcal{T}$ is a subcomplex of $\mathcal{T}$ if $\mathcal{M}$ is a simplicial complex itself. Important classes of subcomplex includes the *star* or *ring* of a simplex. That is for a simplex $\sigma \in \mathcal{T}$

$$\operatorname{star}(\sigma) = \{\tau \in \mathcal{T}, \sigma \subset \tau\}.$$

If two, or more, simplices of $\mathcal{T}$ share a common face, they are called *adjacent* or *neighbors*. The boundary of $\mathcal{T}$ is formed by any proper face that belongs to only one simplex, and its faces.

Associating a set of abstract points with geometric points in $\mathbb{R}^n, n \geq d$, yields a geometric shape composed of piecewise flat simplices. This process is known as the geometric realization of an abstract simplicial complex, or in geometric terms, an embedding of $\mathcal{T}$ into $\mathbb{R}^n$. The embedding hinges on matching abstract and geometric vertices.

It is crucial to distinguish between two aspects of a triangulation $\mathcal{T}$: the topological structure, defined by the connective relationships of vertices, and the geometric shape, determined by the vertices' coordinates. For instance, a planar triangulation is a two-dimensional abstract simplicial complex embeddable in $\mathbb{R}^2$, termed a 2-D triangulation. The same 2-D simplicial complex can also be embedded in $\mathbb{R}^3$, forming a surface triangulation. Despite these different embeddings, both maintain the same combinatorial structure as an abstract simplicial complex, yet they differ in their geometric representation: one as a flat domain in $\mathbb{R}^2$ and the other as a surface in $\mathbb{R}^3$.

3. Linear Finite Element Spaces

In this section we introduce the simplest linear finite element space of $H^1(\Omega)$ and use the scaling argument to estimate the interpolation error. We refer to Exercise 5.4 for an elementary proof using calculus.

3.1. **Linear finite element space and the nodal interpolation.**

Given a shape regular triangulation $\mathcal{T}_h$ of Ω, we set

$$V_h := \{v \,|\, v \in C(\overline{\Omega}), \text{ and } v|_\tau \in \mathcal{P}_1, \forall \tau \in \mathcal{T}_h\},$$

where $\mathcal{P}_1(\tau)$ denotes the space of polynomials of degree 1 (linear) on $\tau \in \mathcal{T}_h$. See Fig. 4 for illustration of linear finite element functions in 1-D and 2-D. Whenever we need to deal with boundary conditions, we further define $V_{h,0} = V_h \cap H_0^1(\Omega)$. We note here that the global continuity is also necessary in the definition of V_h in the sense that if $u \in H^1(\Omega)$, and u is piecewise smooth, then u should be continuous.

We use N to denote the dimension of finite element spaces. For V_h, N is the number of vertices of the triangulation $\mathcal{T}_h$ and for $V_{h,0}$, N is the number of interior vertices. For linear finite element spaces, we have the so called *a nodal basis functions* $\{\phi_i, i = 1, \cdots N\}$ such that ϕ_i is piecewise linear (with respect to the triangulation) and $\phi_i(x_j) = \delta_{i,j}$ for all vertices x_j of $\mathcal{T}_h$. Therefore for any $v_h \in V_h$, we have the representation

$$v_h(x) = \sum_{i=1}^{N} v_h(x_i)\phi_i(x).$$

Due to the shape of the nodal basis function, it is also called the hat function. See Figure 5 for an illustration in 1-D and 2-D. Note that restricting to one simplex, i.e. $\phi_i|_\tau$ is the corresponding barycentrical coordinates.

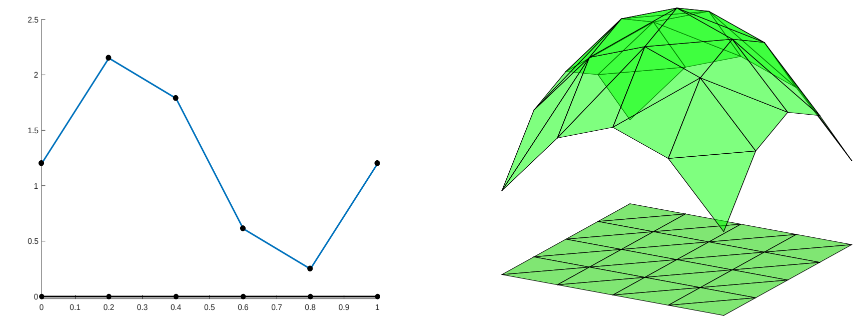

(a) Linear finite element function in 1-D (b) Linear finite element function in 2-D

FIGURE 4. Linear finite element functions

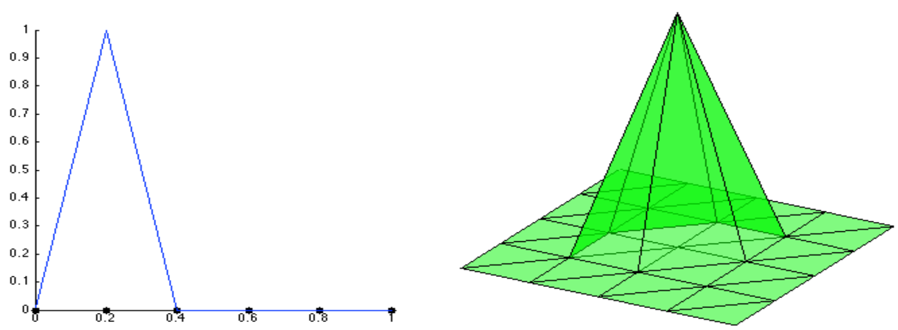

(a) 1-D basis function (b) 2-D basis function

FIGURE 5. Nodal basis (hat) functions in 1-D and 2-D.

The nodal interpolation operator $I_h : C(\overline{\Omega}) \to V_h$ is defined as

$$(I_h u)(x) = \sum_{i=1}^{N} u(x_i)\phi_i(x),$$

and denoted by the short notation $u_I := I_h u$.

3.2. **Scaling argument.** Let $\hat{\tau} = s^n$ be the standard n-simplex which is also called reference simplex. Define an affine map $F : \hat{\tau} \mapsto \tau$, and the function $\hat{v}_h(\hat{x}) = v_h(F(\hat{x})), \forall \hat{x} \in \hat{\tau}$. Essentially it is like a scaling of variables $x = h\hat{x}$ but geometric change is also included in the affine map F consisting of translation, rotation and scaling. The following important relation between the norms on the reference simplex and physical simplex can be easily proved by changing of variable. The shape regularity of a simplex will be needed to bound the 2-norm of Jacobi matrix and its determinant in terms of h.

Lemma 3.1. *When τ is shape regular, we have*

$$\|\hat{D}^\alpha \hat{v}\|_{0,p,\hat{\tau}} \eqsim h_\tau^{\mathrm{sob}_n(k,p)} \|D^\alpha v\|_{0,p,\tau}, \quad \textit{for all} \quad |\alpha| = k, \tag{11}$$

where the Sobolev number is $\mathrm{sob}_n(k,p) = k - \frac{n}{p}$.

Proof. Let $J = \left(\frac{\partial x}{\partial \hat{x}}\right)$ be the Jacobi matrix of the map F. Then $\hat{\nabla}\hat{v} = J\nabla v$ and consequently $|\hat{D}^\alpha \hat{v}| \eqsim h^k |D^\alpha v|$, cf. Exercise 3. Use the change of variable $\mathrm{d}x = |J|\,\mathrm{d}\hat{x} \eqsim h^n\,\mathrm{d}\hat{x}$, we have

$$\int_{\hat{\tau}} |\hat{D}^\alpha \hat{v}|^p \,\mathrm{d}\hat{x} \eqsim \int_\tau h^{kp} |D^\alpha v| h^{-n}\,\mathrm{d}x.$$

Then the results follows. □

For two Banach spaces B_0, B_1, the continuous embedding $B_1 \hookrightarrow B_0$ implies that

$$\|u\|_{B_0} \lesssim \|u\|_{B_1}, \quad \text{for all } \ u \in B_1.$$

The inequality in the reserve way $\|u\|_{B_1} \lesssim \|u\|_{B_0}$ may not true. Now considering finite element spaces $V_h \subset B_i, i = 0, 1$ endowed with two norms. For a fixed h, the dimension of V_h is finite. Since all the norms of finite dimensional spaces are equivalent, there exists constant C_h such that

$$\|u_h\|_{B_1} \leq C_h \|u_h\|_{B_0}, \quad \text{for all } \ u_h \in V_h. \tag{12}$$

The constant C_h in (12) depends on the size and shape of the domain. If we consider the restriction on one element τ and transfer to the reference element $\hat{\tau}$, the constant for the norm equivalence will not depend on h, i.e.,

$$\|\hat{u}_h\|_{B_1,\hat{\tau}} \lesssim \|\hat{u}_h\|_{B_0,\hat{\tau}}.$$

Using the map F, we can then determine the constant in terms of the mesh size h. This is called *scaling argument*.

As an example, we obtain the following typical inverse inequalities

$$|u_h|_{1,\tau} \quad \lesssim \quad h^{-1}\|u_h\|_\tau, \quad \text{and} \tag{13}$$

$$\|u_h\|_{0,p,\tau} \quad \lesssim \quad h^{n(1/p-1/q)}\|u_h\|_{0,q,\tau}, \quad 1 \leq q \leq p \leq \infty. \tag{14}$$

Recall that we have the following refined embedding theorem

$$\|v\|_{0,p,\Omega} \leq C(n,\Omega)\, p^{1-1/n} \|v\|_{1,n,\Omega}, \quad \text{for all } \ 1 \leq p < \infty. \tag{15}$$

Using the inverse inequality and the above embedding result, for $u_h \in V_h$, we have

$$\|v_h\|_\infty \lesssim h^{-n/p}\|v_h\|_{0,p} \lesssim h^{-n/p} p^{1-1/n} \|v_h\|_{1,n}.$$

Now choosing $p = |\log h|$ and noting $h^{-n/|\log h|} \leq C$, we get the following discrete embedding result:

$$\|v_h\|_\infty \lesssim |\log h|^{1-1/n} \|v_h\|_{1,n}, \quad \text{for all } \ v_h \in V_h. \tag{16}$$

In particular, when $n = 2$, we can almost control the maximum norm of a finite element function by its H^1 norm. Although the term $|\log h|$ is unbounded as $h \to 0$, it increases very slowly and appears as a constant for practical h.

3.3. **Error estimate of the nodal interpolation.** We use the scaling argument to estimate the interpolation error $|u - u_I|_{1,\Omega}$ and refer to Exercise 5.4 for a proof using multipoint Taylor series.

Theorem 3.2. *For $u \in H^2(\Omega), \Omega \subset \mathbb{R}^n, n = 1, 2, 3$, and V_h the linear finite element space based on quasi-uniform triangulations $\mathcal{T}_h$, we have*

$$|u - u_I|_{1,\Omega} \lesssim h|u|_{2,\Omega}.$$

Proof. First of all, by the Sobolev embedding theorem, $H^2 \hookrightarrow C(\bar{\Omega})$ for $n \leq 3$. Thus the nodal interpolation u_I is well defined.

Since $|\hat{u}|_{1,\hat{\tau}} \leq \|\hat{u}\|_{2,\hat{\tau}}$, and

$$|\hat{u}_I|_{1,\hat{\tau}} \lesssim \|\hat{u}_I\|_{0,\infty,\hat{\tau}} \leq \|\hat{u}\|_{0,\infty,\hat{\tau}} \lesssim \|\hat{u}\|_{2,\hat{\tau}},$$

we get the estimate in the reference simplex: for $\hat{u} \in H^2(\hat{\tau})$

$$|\hat{u} - \hat{u}_I|_{1,\hat{\tau}} \leq |\hat{u}|_{1,\hat{\tau}} + |\hat{u}_I|_{1,\hat{\tau}} \lesssim \|\hat{u}\|_{2,\hat{\tau}}. \tag{17}$$

The nodal interpolation will preserve linear polynomials i.e. $\hat{p}_I = \hat{p}$ for $\hat{p} \in \mathcal{P}_1(\hat{\tau})$, then

$$|\hat{u} - \hat{u}_I|_{1,\hat{\tau}} = |(\hat{u} + \hat{p}) - (\hat{u} + \hat{p})_I|_{1,\hat{\tau}} \lesssim \|\hat{u} + \hat{p}\|_{2,\hat{\tau}},\ \forall\, \hat{p} \in \mathcal{P}_1(\hat{\tau}),$$

and thus by the Bramble-Hilbert lemma

$$|\hat{u} - \hat{u}_I|_{1,\hat{\tau}} \lesssim \inf_{\hat{p} \in \mathcal{P}_1(\hat{\tau})} \|\hat{u} + \hat{p}\|_{2,\tau} \lesssim |\hat{u}|_{2,\hat{\tau}}. \tag{18}$$

We now use the scaling argument to transfer the inequality back to the simplex τ. First

$$|\hat{u}|_{2,\hat{\tau}} \lesssim h_\tau^{2-\frac{n}{2}} |u|_{2,\tau}.$$

To scale the left hand side, we need a property of the interpolation operator

$$\widehat{u - u_I} = \hat{u} - \hat{u}_I, \tag{19}$$

namely the interpolation is affine invariant, which can be verified easily by definition. Then by the scaling argument

$$h_\tau^{1-\frac{n}{2}} |u - u_I|_{1,\tau} \lesssim |\widehat{u - u_I}|_{1,\hat{\tau}} = |\hat{u} - \hat{u}_I|_{1,\hat{\tau}}.$$

Combing all the arguments above leads to the interpolation error estimate on a quasiuniform mesh. For $u \in H^2(\Omega)$,

$$|u - u_I|_{1,\Omega}^2 = \sum_{\tau \in \mathcal{T}_h} |u - u_I|_{1,\tau}^2 \lesssim \sum_{\tau \in \mathcal{T}_h} h_\tau^2 |u|_{2,\tau}^2 \eqsim h^2 |u|_{2,\Omega}^2.$$

□

4. CONVERGENCE ANALYSIS

Finite element methods for solving Poisson equation is a special case of Galerkin method by choosing the subspace $V_h \subset V$ based on a triangulation $\mathcal{T}_h$ of the underlying domain. As an example, let us consider the linear finite element space V_h. The finite element approximation will be: find $u_h \in V_h$ such that

$$a(u_h, v_h) = \langle f, v_h \rangle, \quad \text{for all } \ v_h \in V_h. \tag{20}$$

Again the existence and uniqueness follows from the Riesz representation theorem since $f \in V' \subset V_h'$ is also a continuous linear functional on V_h and by Poincaré inequality $a(\cdot,\cdot)$ defines an inner production on $H_0^1(\Omega)$.

4.1. H^1 **error estimate.** We first derive an important orthogonality result for projections. Let u and u_h be the solution of continuous and discrete equations respectively i.e.

$$a(u,v) = \langle f, v\rangle \qquad \forall v \in H_0^1(\Omega),$$
$$a(u_h,v) = \langle f, v\rangle \qquad \forall v \in V_h.$$

Choosing $v \in V_h$ in both equations and subtracting them, we then get an important orthogonality

$$a(u-u_h, v_h) = 0 \qquad \forall v_h \in V_h, \tag{21}$$

which implies the following optimality of the finite element approximation

$$\|\nabla(u-u_h)\| = \inf_{v_h\in V_h} \|\nabla(u-v_h)\|. \tag{22}$$

Theorem 4.1. *Let u and u_h be the solution of continuous and discrete equations respectively. When $u \in H^2(\Omega)\cap H_0^1(\Omega)$, we have the following optimal order estimate:*

$$\|\nabla(u-u_h)\| \lesssim h\|u\|_2. \tag{23}$$

Furthermore when H^2-regularity result holds, we have

$$\|\nabla(u-u_h)\| \lesssim h\|f\|. \tag{24}$$

Proof. When $u \in H^2(\Omega)\cap H_0^1(\Omega)$, the nodal interpolation operator is well defined by the embedding theorem. By (22), we then have

$$\|\nabla(u-u_h)\| \le \|\nabla(u-u_I)\| \lesssim h\|u\|_2 \lesssim h\|f\|.$$

Here in the second $\lesssim$, we have used the error estimate of interpolation operator, and in the third one, we have useed the regularity result. □

4.2. L^2 **error estimate.** Now we estimate $\|u-u_h\|$. The main technical is the combination of the duality argument and the regularity result. It is known as Aubin-Nitsche duality argument or simply "Nitsche's trick".

Theorem 4.2. *Let u and u_h be the solution of continuous and discrete equations respectively. Suppose the H^2 regularity result holds, we then have the following optimal order approximation in L^2 norm*

$$\|u-u_h\| \lesssim h^2\|u\|_2. \tag{25}$$

Proof. By the H^2 regularity result, there exists $w \in H^2(\Omega)\cap H_0^1(\Omega)$ such that

$$a(w,v) = (u-u_h, v), \quad \text{for all } \ v \in H_0^1(\Omega), \tag{26}$$

and $\|w\|_2 \le C\|u-u_h\|$. Choosing $v = u-u_h$ in (26), we get

$$\begin{aligned}
\|u-u_h\|^2 &= a(w, u-u_h)\\
&= a(w-w_I, u-u_h)\\
&\le \|\nabla(w-w_I)\|\|\nabla(u-u_h)\| && \text{(orthogonality)}\\
&\lesssim h\|w\|_2\|\nabla(u-u_h)\|\\
&\lesssim h\|u-u_h\|\|\nabla(u-u_h)\| && \text{(regularity).}
\end{aligned}$$

Canceling one $\|u-u_h\|$, we get

$$\|u-u_h\| \le Ch\|\nabla(u-u_h)\| \lesssim h^2\|u\|_2.$$

□

For the estimate in H^1 norm, when u is smooth enough, we can obtain the optimal first order estimate. But for L^2 norm, the duality argument requires H^2 elliptic regularity, which in turn requires that the polygonal domain be convex. In fact, for a non-convex polygonal domain, it will usually not be true that $\|u - u_h\| = \mathcal{O}(h^2)$ even if the solution u is smooth.

5. Exercise

Exercise 5.1. In this exercise, we calculate integrals using barycentric coordinate. For an $n+1$ multi-index α and an n-simplex τ, one has

$$\int_\tau \boldsymbol{\lambda}^\alpha(\boldsymbol{x}) d\boldsymbol{x} = \frac{\alpha! n!}{(|\alpha| + n)!} |\tau|. \tag{27}$$

A multi-index α is an k-tuple of non-negative integers $\alpha = (\alpha_1, \alpha_2, \cdots, \alpha_k)$. The length of α is defined by $|\alpha| = \sum_{i=1}^k \alpha_i$, and $\alpha! = \alpha_1! \ldots \alpha_n!$. For a given vector $\boldsymbol{x} = (x_1, x_2, \cdots, x_k)$, we define $\boldsymbol{x}^\alpha = x_1^{\alpha_1} x_2^{\alpha_2} \cdots x_k^{\alpha_k}$. Finally let $\boldsymbol{\lambda} = (\lambda_1, \lambda_2, \cdots, \lambda_{n+1})$ denote the vector of barycentric coordinates.

We shall prove the identity (27) through the following sub-problems:

(1) $n = 1$ and $\tau = [0, 1]$. Prove that
$$\int_0^1 x^{\alpha_1} (1 - x)^{\alpha_2} dx = \frac{\alpha_1! \alpha_2!}{(\alpha_1 + \alpha_2 + 1)!}$$
(2) $n = 2$ and $\tau = s^2$. Prove that
$$\int_\tau x^{\alpha_1} y^{\alpha_2} (1 - x - y)^{\alpha_3} dx = \frac{\alpha_1! \alpha_2! \alpha_3!}{(\alpha_1 + \alpha_2 + \alpha_3 + 2)!}$$
(3) Prove the identity (27) for $\tau = s^n$ using induction on n.
(4) Prove the identity (27) for general simplex τ by using the transformation from the standard simplex s^n.

Exercise 5.2. In this exercise, we give explicit formula of the stiffness matrix in a triangle. Let τ be a triangle with vertices $\boldsymbol{x}_1, \boldsymbol{x}_2, \boldsymbol{x}_3$ and let $\lambda_1, \lambda_2, \lambda_3$ be corresponding barycentric coordinates.

(1) Let $\boldsymbol{n}_i$ be the outward normal vector of the edge e_i and d_i be the distance from $\boldsymbol{x}_i$ to e_i. Prove that
$$\nabla \lambda_i = -\frac{1}{d_i} \boldsymbol{n}_i.$$
(2) Let θ_i be the angle associated to the vertex $\boldsymbol{x}_i$. Prove that
$$\int_\tau \nabla \lambda_i \cdot \nabla \lambda_j \, \mathrm{d}x = -\frac{1}{2} \cot \theta_k,$$
where (i, j, k) is any permutation of $(1, 2, 3)$.
(3) Let $c_i = \cot \theta_i, i = 1$ to 3. If we define the local stiffness matrix $\boldsymbol{A}_\tau$ as 3×3 matrix formed by $\int_\tau \nabla \lambda_i \cdot \nabla \lambda_j \, dx, i, j = 1, 2, 3$. Show that
$$\boldsymbol{A}_\tau = \frac{1}{2} \begin{bmatrix} c_2 + c_3 & -c_3 & -c_2 \\ -c_3 & c_3 + c_1 & -c_1 \\ -c_2 & -c_1 & c_1 + c_2 \end{bmatrix}.$$

(4) Let e be an interior edge in the triangulation $\mathcal{T}$ with nodes x_i and x_j, and shared by two triangles τ_1 and τ_2. Denoted the angle in τ oppositing to e by θ_e^τ. Then prove that the entry $a_{ij} = \int_\Omega \nabla \phi_i \cdot \nabla \phi_j \, dx$ is

$$a_{ij} = -\frac{1}{2}(\cot \theta_e^{\tau_1} + \cot \theta_e^{\tau_2}).$$

Consequently $a_{ij} \leq 0$ if and only if $\theta_e^{\tau_1} + \theta_e^{\tau_2} \leq \pi$. By the way, if a 2-D triangulation satisfying $\theta_e^{\tau_1} + \theta_e^{\tau_2} \leq \pi$, it is called a Delaunay triangulation.

Exercise 5.3. In this exercise, we compute the singular values of the affine map from the reference triangle $\hat{\tau}$ spanned by $\hat{a}_1 = (1,0), \hat{a}_2 = (0,1)$ and $\hat{a}_3 = (0,0)$ to a triangle τ with three vertices $a_i, i = 1,2,3$. One of such affine map is to match the local indices of three vertices, i.e., $F(\hat{a}_i) = a_i, i = 1,2,3$:

$$F(\hat{\boldsymbol{x}}) = B^{\intercal}(\hat{\boldsymbol{x}}) + c,$$

where

$$B = \begin{bmatrix} x_1 - x_3 & y_1 - y_3 \\ x_2 - x_3 & y_2 - y_3 \end{bmatrix}, \text{ and } c = (x_3, y_3)^{\intercal}.$$

(1) Estimate the $\sigma_{\max}(B)$ and $\sigma_{\min}(B)$ in terms of edge lengthes and angles of the triangle τ.
(2) Establish inequalities between $\|\nabla v\|_{0,\tau}$ and $\|\hat{\nabla} \hat{v}\|_{0,\hat{\tau}}$ where $\hat{v}(\hat{x}) := v(F(\hat{x}))$.

Exercise 5.4. In this exercise, we give a proof of the interpolation error estimate using calculus. Let τ be a simplex with vertices $\boldsymbol{x}_i, i = 1, \ldots, n+1$ and $\{\lambda_i, i = 1, \ldots, n+1\}$ be the corresponding barycentric coordinates.

(1) Show that

$$u_I(\boldsymbol{x}) = \sum_{i=1}^{n+1} u(\boldsymbol{x}_i)\lambda_i(\boldsymbol{x}), \quad \sum_{i=1}^{n+1} \lambda_i(\boldsymbol{x}) = 1, \quad \text{and} \quad \sum_{i=1}^{n+1}(\boldsymbol{x} - \boldsymbol{x}_i)\lambda_i(\boldsymbol{x}) = 0.$$

(2) Let us introduce the auxiliary functions

$$g_i(t, \boldsymbol{x}) = u(\boldsymbol{x}_i + t(\boldsymbol{x} - \boldsymbol{x}_i)).$$

For $u \in C^2(\bar{\tau})$, prove the following error equations

$$(u_I - u)(\boldsymbol{x}) = \sum_{i=1}^{n+1} \lambda_i(\boldsymbol{x}) \int_0^1 t g_i''(t, \boldsymbol{x}) dt,$$

$$\nabla(u_I - u)(\boldsymbol{x}) = \sum_{i=1}^{n+1} \nabla \lambda_i \int_0^1 t g_i''(t, \boldsymbol{x}) dt.$$

Hint: Multiply the following Taylor series by λ_i and sum over i

$$g_i(0, \boldsymbol{x}) = g_i(1, \boldsymbol{x}) - g_i'(1, \boldsymbol{x}) + \int_0^1 t g_i''(t, \boldsymbol{x}) dt.$$

(3) Let $u \in W^{2,p}$ with $p > n/2$. Using the error formulate in (2) to prove

$$\|u - u_I\|_{0,p} \leq C_1 h^2 |u|_{2,p}, \quad |u - u_I|_{1,p} \leq C_2 h |u|_{2,p}.$$

Try to obtain sharp constants in the above inequalities.